Journal of Neurochemistry, 2007, **101**, 1619–1631 doi:10.1111/j.1471-4159.2007.04516.x

'Mild Uncoupling' does not decrease mitochondrial superoxide levels in cultured cerebellar granule neurons but decreases spare respiratory capacity and increases toxicity to glutamate and oxidative stress

L. I. Johnson-Cadwell, M. B. Jekabsons,[1] A. Wang, B. M. Polster and D. G. Nicholls

Buck Institute for Age Research, Novato, California, USA

Abstract

Cultured rat cerebellar granule neurons were incubated with low nanomolar concentrations of the protonophore carbonyl-cyanide-p-trifluoromethoxyphenyl hydrazone (FCCP) to test the hypothesis that 'mild uncoupling' could be neuroprotective by decreasing oxidative stress. To quantify the uncoupling, respiration and mitochondrial membrane potential ($\Delta\psi_m$) were determined in parallel as a function of FCCP concentration. $\Delta\psi_m$ dropped by less than 10 mV before respiratory control was lost. Conditions for the valid estimation of matrix superoxide levels were determined from the rate of oxidation of the matrix-targeted fluorescent probe MitoSOX. No significant change in the level of matrix superoxide could be detected on addition of FCCP while respiratory control was retained, although cytoplasmic superoxide levels measured by dihydroethidium oxidation increased. 'Mild uncoupling' by 30 nmol/L FCCP did not alleviate neuronal dysregulation induced by glutathione depletion and significantly enhanced that due to menadione-induced oxidative stress. Low protonophore concentrations enhanced *N*-methyl-D-aspartate receptor-induced delayed calcium deregulation consistent with a decrease in the spare respiratory capacity available to match the bioenergetic demand of chronic receptor activation. It is concluded that the 'mild uncoupling' hypothesis is not supported by this model.

Keywords: calcium, glutamate, mitochondria, mitochondrial membrane potential, oxidative stress, superoxide.

J. Neurochem. (2007) **101**, 1619–1631.

'Mild uncoupling', i.e., the enhancement of the natural proton conductance of the inner mitochondrial membrane (C_mH^+) has been proposed as a protective mechanism in neurons and other cells, lowering the mitochondrial membrane potential ($\Delta\psi_m$) and thus alleviating oxidative stress [reviewed in Brand *et al.* (2004); Rousset *et al.* (2004); Horvath *et al.* (2003); Nedergaard and Cannon (2003); Andrews *et al.* (2005a)]. The hypothesis is based on two observations; first, levels of reactive oxygen species such as superoxide ($O_2^{\cdot -}$) generated by isolated mitochondria oxidizing succinate and other substrates that bypass Complex I are very sensitive to protonophore-induced decreases in $\Delta\psi_m$ (Korshunov *et al.* 1997; Votyakova and Reynolds 2001; Lambert and Brand 2004). Secondly, many cells including neurons express low levels of novel uncoupling proteins or nUCPs with sequence homology to the brown adipose tissue uncoupling protein (UCP1) and these are proposed to play a similar mild uncoupling role in intact cells. While there is significant phenomenological support for this hypothesis (Diano *et al.* 2003; Mattiasson *et al.* 2003; Andrews *et al.* 2005b; Conti *et al.* 2005) there remain many unanswered questions concerning the dependency of $O_2^{\cdot -}$ on $\Delta\psi_m$ in intact cells where mitochondria oxidize predominantly

Received September 6, 2006; revised manuscript received December 13, 2006; accepted December 18, 2006.

Address correspondence and reprint requests to David G. Nicholls, Buck Institute for Age Research, 8001 Redwood Boulevard, Novato, CA 94945, USA. E-mail: dnicholls@buckinstitute.org

[1]The present address of M.B. Jekabsons is the Department of Biology, 110 Shoemaker Hall, University of Mississippi, MS 38677, USA.

Abbreviations used: CGN, cerebellar granule neuron; C_mH^+, inner mitochondrial membrane proton conductance; DCD, delayed Ca^{2+} deregulation; DHE, dihydroethidium; FCCP, carbonylcyanide-p-trifluoromethoxyphenyl hydrazone; MK-801, {(+)-5-methyl-10,11-dihydro-5H-dibenzo[a,d]cyclohepten-5,10-imine maleate; MnTE-2-PyP, manganese tetrakis (N-ethylpyridinium-2yl) porphyrin; NMDA, *N*-methyl-D-aspartate; nUCP, novel uncoupling protein; $O_2^{\bullet -}$, superoxide anion; $TMRM^+$, tetramethylrhodamine methyl ester; UCP1, uncoupling protein 1; ΔpH, pH gradient across the inner mitochondrial membrane; $\Delta\psi_m$, mitochondrial membrane potential; $\Delta\psi_p$, plasma membrane potential.

NADH-linked substrates such as, the capacity and activation status of the nUCPs (Nicholls 2006b), and the consequence of the increased C_mH^+ on the ability of the mitochondria to generate ATP.

Because of uncertainty as to the physiological activation mechanism of the nUCPs (Nicholls 2006b) and whether they even possess protonophoric activity (Nicholls 2006b) we have modeled the putative nUCP-mediated uncoupling by investigating the effects of low protonophore concentrations on the inner membrane proton conductance, respiratory stimulation, spare respiratory capacity, mitochondrial depolarization, matrix and cytoplasmic superoxide levels and susceptibility to oxidative stress and to glutamate excitoxicity of cultured rat cerebellar granule neurons (CGNs) under conditions of maximal N-methyl-D-aspartate (NMDA) receptor activation.

We have previously shown that acute glutathione depletion of CGNs induces oxidative changes to the mitochondria that inhibit the export of ATP to the cytoplasm and facilitate spontaneous and glutamate-induced delayed Ca^{2+} deregulation (DCD, the first irreversible step in necrotic cells death) (Vesce *et al.* 2005). Similarly, the superoxide generated at the mitochondria by redox cycling of menadione facilitates DCD (Nicholls *et al.* 1998). The mild uncoupling hypothesis would predict that low protonophore concentrations would provide a measure of protection against these oxidative stresses.

In contrast, while oxidative stress is implicated in the excitotoxic death of neurons exposed to chronic NMDA receptor activation [for reviews see Coyle and Puttfarcken (1993); Beal (1995); Rego and Oliveira (2003); Beal (1996)] the consensus view that Ca^{2+} entry into the neuron and its accumulation by mitochondria leads to increased superoxide levels that promote necrotic cell death (Dugan *et al.* 1995; Reynolds and Hastings 1995; Sengpiel *et al.* 1998) is contradicted by our studies indicating that observed increases in $O_2^{\cdot-}$ levels during excitotoxic glutamate exposure are a consequence and not a cause of DCD (Vesce *et al.* 2004). 'Mild uncoupling' would not therefore be predicted to protect against glutamate-induced DCD. Instead, since Ca^{2+} and Na^+ entry through the activated NMDA receptor imposes a heavy ATP demand on the neuron for the re-extrusion of the cations (Jekabsons and Nicholls 2004), the inevitable decrease in mitochondrial ATP generating capacity resulting from the increased proton leak could initiate an 'ATP crisis' in the cell facilitating cell death. This is seen in the present study. Taking these results together, it is difficult to understand how a physiological uncoupling mechanism during oxidative or excitotoxic stress could be neuroprotective.

Materials and methods

Reagents

MitoSOX Red, fluo-5 F, fluo-4FF, Mitotracker Green and dihydroethidine were purchased from Molecular Probes (Eugene, OR, USA). Manganese tetrakis (*N*-ethylpyridinium-2yl) porphyrin (MnTE-2-PyP) was a gift from Dr Manisha Patel. All other reagents were from Sigma–Aldrich (St Louis, MO, USA).

Culture and incubation of cerebellar granule neurons

Wistar rat CGNs were prepared as previously described (Courtney *et al.* 1990) with modifications. In brief, cells were plated onto coverslip-based 8-well chambers (LabTek, Naperville, IL, USA) previously coated with 33 μg/mL polyethleneimine, at a density of 380 000 cells per 0.8 cm^2 well for confocal imaging experiments, or on 22×40 mm coverslips at a density of 3×10^6 cells for respiration determination. Cultures were maintained in minimal essential medium supplemented with 10% fetal bovine serum, 30 mmol/L glucose, 20 mmol/L KCl, 2 mmol/L glutamine, 50 units/mL penicillin and 50 μg/mL streptomycin. 24 h after plating, 10 μmol/L cytosine arabinoside was added to inhibit growth of non-neuronal cells. Cell cultures were maintained at 37°C in an incubator with humidified atmosphere of 5% CO_2/95% air and used for experiments after 7–8 days in culture. Cells were washed and experiments performed in incubation medium (3.5 mmol/L KCl, 120 mmol/L NaCl, 1.3 mmol/L $CaCl_2$, 0.4 mmol/L KH_2PO_4, 5 mmol/L $NaHCO_3$, 1.2 mmol/L Na_2SO_4, 15 mmol/L D-glucose and 20 mmol/L Na-Tes, pH 7.4, 37°C) with further additions as detailed.

In situ respirometry

Cells cultured on rectangular coverslips were assembled into a Warner Instruments (Harndon, CT, USA) RC-30 closed imaging chamber and mounted on an Olympus (Center Valley, PA, USA) IX 70 inverted fluorescence microscope. The chamber was perfused with incubation medium at 50 μL/min and the downstream depletion in oxygen content monitored with a miniature Clark-type oxygen electrode as previously described (Jekabsons and Nicholls 2004). Where indicated the perfusion medium was supplemented with nanomolar concentrations of FCCP.

Functional imaging

Cells were imaged on a Zeiss (Thornwood, NY, USA) Pascal Confocal Axiovert 100 mol/L microscope. Images were collected using a 20× air or a 63× oil objective. A custom built acrylic chamber enclosed the entire microscope stage, allowing the temperature of the objectives and cells to be maintained at 37°C.

In situ mitochondrial membrane potentials

Cerebellar granule neurons were equilibrated with 5 nmol/L tetramethylrhodamine methyl ester ($TMRM^+$) in incubation medium for 60 min with the addition of 1 μmol/L tetraphenylboron to facilitate equilibration across the plasma membrane (Ward *et al.* 2000). This concentration of $TMRM^+$ is insufficient for dye aggregation to occur within the mitochondrial matrix and in this mode it is important to correct for changes in plasma membrane potential, $\Delta\psi_p$. However, in a previous study utilizing a simultaneous fluorescent anion to monitor $\Delta\psi_p$ (Nicholls 2006a) plasma membrane potential was found to change by less than 2 mV on addition of 250 nmol/L FCCP or respiratory chain inhibitors and hence the anion indicator was omitted in the present study. Changes in $\Delta\psi_m$ were quantified from changes in $TMRM^+$ fluorescence using a computer simulation (Nicholls 2006a) with the constants previ-

ously determined for CGNs incubated under the present conditions. Cells were excited in single-track mode with the 514 mm band of an argon laser. Emission was determined with a 595–650 nm filter.

Delayed calcium deregulation

For experiments in which DCD was monitored following oxidative stress, 13DIV CGNs were equilibrated with incubation buffer containing additionally 0.5 μmol/L fluo-4FF-AM and 10 nmol/L $TMRM^+$ plus 1 μmol/L tetraphenylboron. Cells were then exposed to 300 μmol/L menadione or 100 μmol/L monochlorobimane. Regions of interest were defined to encompass the entire field of ~100 neurons and the time-course of decrease in $TMRM^+$ fluorescence (reflecting plasma and/or mitochondrial depolarization) and increase in fluo-4FF fluorescence (reflecting DCD) was determined in three independent experiments. For glutamate excitotoxicity cells were pre-incubated with 0.5 μmol/L Fluo4FF and exposed to 200 μmol/L glutamate, 20 μmol/L glycine in the presence of differing FCCP concentrations. DCD was monitored by the increase in fluorescence in the entire field as above.

Calculation of effective proton conductance (C_mH^+) of *in situ* mitochondria

C_mH^+ was calculated by determining the proton flux through the inner mitochondrial membrane from the respiratory rates multiplied by 10 for the estimated stoichiometry of proton extrusion by the respiratory chain for Complex I substrates (Brand 2005). This value was then divided by the estimated $\Delta\psi_m$. Note that the conductance is the sum of that due to the ATP synthase, the endogenous proton leak and the added protonophore.

Subcellular localization of the oxidation products of dihydroethidium and MitoSOX

MitoSOX Red dissolved in DMSO was used at a final concentration not exceeding 0.2 μmol/L to avoid saturation of the mitochondrial signal within the time-course of the experiment and the consequent appearance of excess fluorescent oxidation product (termed here 'Mitoethidium') bound to nuclear DNA. CGNs were washed and incubation buffer added. The probe was added to the cells immediately at the start of each experiment and images in the focal plane of the cell bodies or neurites captured with the Zeiss confocal using a 63× oil-immersion objective. In order to monitor whole-cell (rather then mitochondrial) superoxide levels, cells were incubated in the standard incubation buffer with 0.1 μmol/L dihydroethidium (DHE) reconstituted in DMSO added at the start of each experiment. In order to remove any ethidium formed by prior spontaneous oxidation Dowex cation exchange beads were added to the DHE stock for 30 min immediately prior to use.

In situ mitochondrial and whole-cell superoxide levels

The fluorescence time-course was determined in single cell CGN somata incubated with MitoSOX Red at 0.1 or 0.2 μmol/L (unless otherwise stated) using a 20× air objective (excitation 543 nm emission 595–650 nm). As MitoSOX is a lipid-permeant cation it was assumed that it distributes across plasma and mitochondrial membranes in a similar way to $TMRM^+$, i.e., responsive to changes in plasma or mitochondrial membrane potential. It should be noted that the oxidized 'Mitoethidium' will carry two positive charges. Where appropriate the rate of MitoSOX oxidation was corrected for predicted changes in its matrix concentration determined from parallel $TMRM^+$ determinations using the computer simulation in Nicholls 2006a. Briefly, the depolarization calculated from the $TMRM^+$ fluorescence was used to calculate the decreased accumulation of MitoSOX in the matrix. Because the rate of oxidation of MitoSOX is proportional to its matrix concentration the slope of the fluorescence trace in experiments with sub-optimal $\Delta\psi_m$ were increased to compensate for the lowered MitoSOX concentration. This correction was considered insufficiently accurate for large mitochondrial depolarizations induced by high protonophore concentrations.

MitoSOX and isolated mitochondria

Mouse liver mitochondria (0.25 mg protein/mL) obtained by conventional differential centrifugation (Lambert and Brand 2004) were incubated in medium containing 125 mmol/L KCl, 2 mmol/L K_2HPO_4, 20 mmol/L HEPES, 5 mmol/L malate, 5 mmol/L pyruvate, 4 mmol/L $MgCl_2$, 3 mmol/L ATP and 50 μmol/L EGTA, 37°C, pH 7.0 in a stirred microcuvette within a Perkin-Elmer LS55 spectrofluorimeter, excitation 477–492 nm, emission 570–590 nm. 10 μmol/L MitoSOX was added and allowed to equilibrate for 5 min before starting recording.

Results

Cerebellar granule neuron respiration and $\Delta\psi_m$ in the presence of FCCP

When isolated mitochondria are titrated with protonophore (Nicholls and Bernson 1977) there is an initial increase in respiration with only a slight drop in $\Delta\psi$. However, once uncontrolled respiration is attained, the inability of the respiratory chain to compensate for a further increase in conductance by enhancing proton extrusion means that $\Delta\psi$ falls sharply (Nicholls and Bernson 1977). It is therefore important not to exceed the concentration at which respiratory control is lost in order to simulate a physiological protonophoric conductance. The development of a 'cell respirometer' to quantify the respiration of coverslip-attached neurons (Jekabsons and Nicholls 2004) allows such a titration to be quantified. Fig. 1 shows that the CGNs retain respiratory control up to 100 nmol/L FCCP. However, with each addition the 'spare respiratory capacity' decreases. 250 nmol/L FCCP (not shown) was sufficient to induce uncontrolled respiration. Fig. 2a monitors the drops in $\Delta\psi_m$ (quantified by the computer program in Nicholls 2006a) that are induced by FCCP in parallel experiments. A substantial drop in $\Delta\psi_m$ is only seen when respiration can no longer accelerate to compensate for the increased proton leak (i.e., at 250 nmol/L or 750 nmol/L FCCP). Importantly, FCCP concentrations that give substantial increases in respiration in Fig. 1 (10–100 nmol/L) produced decreases in $\Delta\psi_m$ that are almost below the level of detection (2–5 mV calculated from the computer simulation). The ability to monitor $\Delta\psi_m$ and respiration in parallel allows the inner membrane effective proton conductance, C_mH^+, to be calculated as a function of

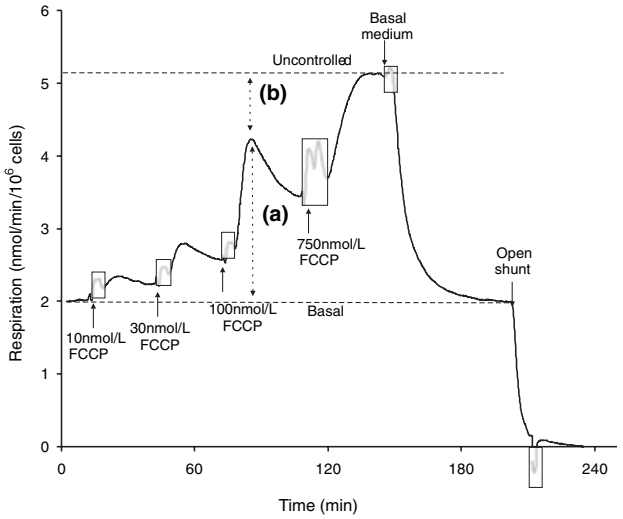

Fig. 1 Cerebellar granule neuron (CGN) respiration as a function of carbonylcyanide-p-trifluoromethoxyphenyl hydrazone (FCCP) concentration. CGNs (3×10^6 cells) were perfused with incubation buffer in the cell respirometer (see Materials and methods). Where indicated by the arrows the perfusion was switched to media containing the indicated concentrations of FCCP. At the end of the experiment, a bypass shunt was opened to control for drift and to detect any cell death. The grayed boxes represent flow artifacts associated with the change in perfusate. (a) FCCP-induced respiratory stimulation; (b) residual respiratory capacity.

protonophore concentration by the application of 'Ohm's Law', i.e., the respiratory rate multiplied by the H^+/O stoichiometry (taken here to be 10) gives the proton current, and this divided by the membrane potential gives the proton conductance (Fig. 2b). The linear relationship is similar to that previously published for isolated mitochondria (Nicholls and Bernson 1977) except that the slope is shallower. The intercept with the *y*-axis gives the basal proton conductance of the inner membrane (including proton re-entry through the ATP synthase).

The rate of electron transfer in the respiratory chain is a roughly linear function of the disequilibrium between the redox potential spans through Complexes I and III and the free energy required to pump protons against the existing $\Delta\psi$, or strictly the protonmotive force (Nicholls and Bernson 1977). The slope of the relationship between $\Delta\psi_m$ and respiration reflects the 'internal resistance' of the respiratory chain proton pumps, i.e., the magnitude of the thermodynamic disequilibrium between the redox span and the protonmotive force required for a given flux. Fig. 2c shows

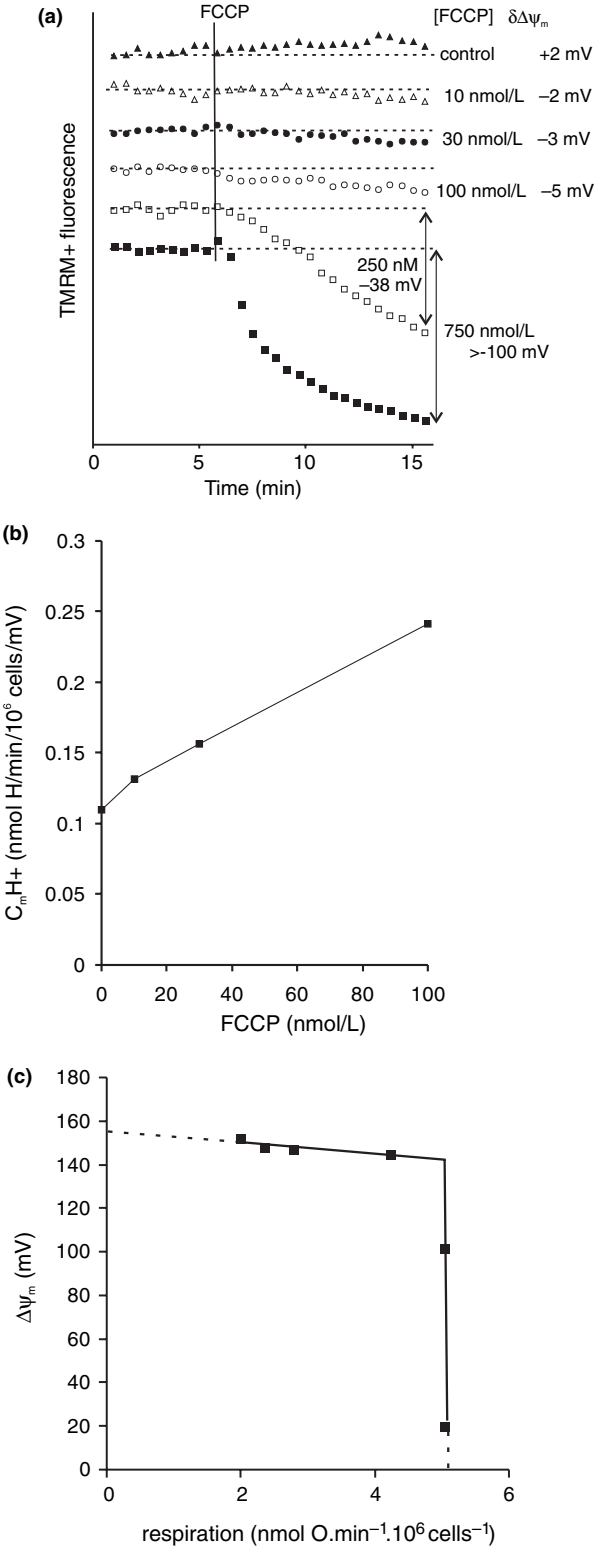

Fig. 2 $\Delta\psi_m$ and C_mH^+ of *in situ* mitochondria as a function of carbonylcyanide-p-trifluoromethoxyphenyl hydrazone (FCCP) concentration. (a) $TMRM^+$ fluorescence and calculated change in mitochondrial membrane potential ($\delta\Delta\psi_m$) for cerebellar granule neurons in incubation medium as a function of added FCCP. Note that $\Delta\psi_m$ in the presence of 250 nmol/L FCCP was still falling at the termination of the experiment. Traces are displaced vertically for clarity. (b) Effective proton conductance of *in situ* mitochondria as a function of added FCCP. (c) Variation of $\Delta\psi_m$ with respiratory rate as FCCP is increased. For details see Materials and methods.

that the change in $\Delta\psi_m$ with respiratory rate is very small, suggesting that a slight thermodynamic disequilibrium in the complexes supports a rapid electron flux. Although changes in ΔpH were not determined, this immediately suggests that any decrease in $\Delta\psi_m$ to restrict superoxide generation can only be bought at a substantial cost in terms of reserve ATP generating capacity, which cannot exceed that driven by the residual spare respiratory capacity, e.g., 'b' in Fig. 1.

Characterization of MitoSOX oxidation as a monitor of mitochondrial matrix superoxide levels

MitoSOX is a derivative of DHE conjugated to triphenylphosphonium that confers a positive charge leading to its accumulation within the mitochondrial matrix. MitoSOX can detect the increased levels of matrix superoxide in isolated mitochondria with Complex III inhibition by antimycin A (Fig. 3). As is the case for ethidium (the oxidation product of DHE), the fluorescence of the oxidized 'mitoethidium' is enhanced by intercalation into nucleic acids. It is therefore important for cell studies that the binding capacity of mitochondrial nucleic acids is not exceeded, as otherwise a non-linear response could result. Fig. 4a shows the time course of fluorescence development in single cell bodies (mean signal from 10 cell somata) when CGNs were continuously exposed to MitoSOX from 10 to 500 nmol/L. A linear increase with time was observed for concentrations from 10 to 100 nmol/L over a time range from 30 to 90 min following probe addition. Importantly, the rate of increase in fluorescence over this range was a linear function of the external MitoSOX concentration, and hence of its concentration in the matrix (Fig. 4b). As MitoSOX is a membrane-permeant cation, it should distribute across the plasma and mitochondrial membranes in response to $\Delta\psi_p$ and $\Delta\psi_m$ in a similar way to membrane potential probes such as $TMRM^+$. This in turn raises a complication in the use of the probe, namely that a change in either potential will influence the sensitivity of the probe as a detector of matrix superoxide

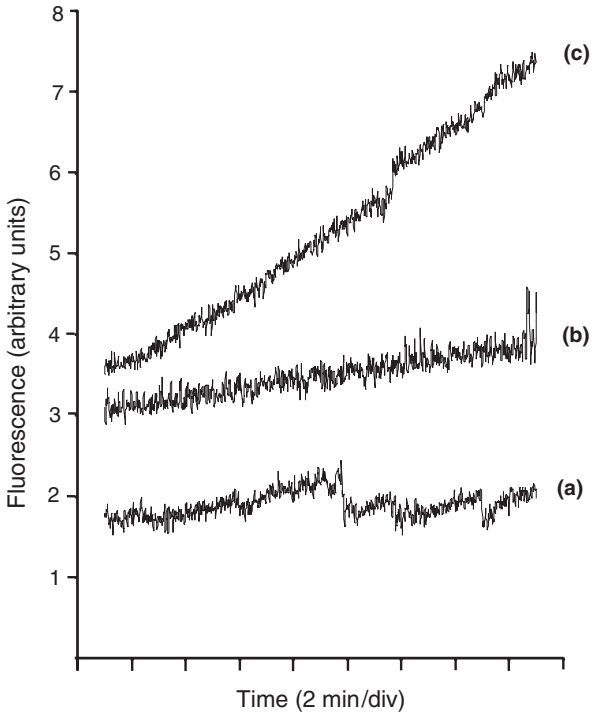

Fig. 3 Detection of antimycin A-induced superoxide levels in the matrices of isolated mouse liver mitochondria. Mitochondria were incubated in the presence of pyruvate and malate. (a) Autofluorescence was monitored in the absence of antimycin A or MitoSOX. (b) Fluorescence changes were determined after a 5 min preincubation with MitoSOX. (c) The experiment was repeated in the presence of MitoSOX and 2 μmol/L antimycin A (added 5 min prior to the start of recording).

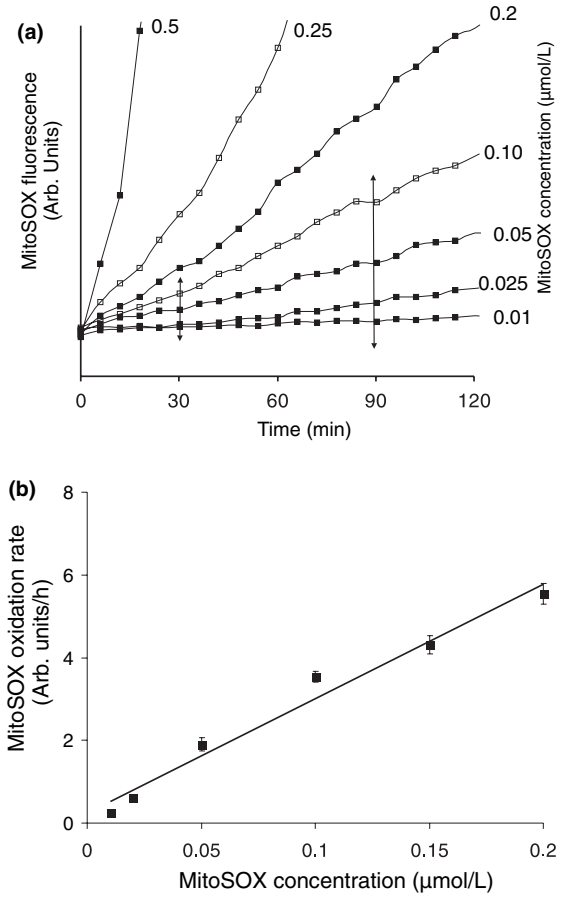

Fig. 4 Characterization of MitoSOX oxidation and fluorescence in cerebellar granule neurons (CGNs) equilibrated with varying probe concentrations: (a) CGNs were equilibrated with concentrations of MitoSOX from 10 nmol/L to 0.5 μmol/L and the increase in fluorescence monitored (each point is the mean of 10 somata). (b) Over the period from 30 min to 90 min after addition of the probe, the rate of fluorescence increase was a linear function of the MitoSOX concentration in the incubation medium. Error bars reflect the standard deviation of the slope in the representative experiment in (a).

levels by altering its concentration in the matrix. Equilibration of the cells with concentrations of MitoSOX in excess of 0.25 μmol/L resulted in the appearance of nuclear fluorescence (data not shown).

To compare the location of Mitoethidium with ethidium produced by oxidation of DHE, CGNs were labeled with Mitotracker Green and incubated with MitoSOX or DHE (Fig. 5). A close co-localization of the Mitoethidium fluorescence with Mitotracker was seen in healthy cells (Fig. 5a), although nuclear labeling was evident in damaged cells (which were not included in the subsequent analyses). In contrast, DHE produced extensive nuclear ethidium labeling in all cell bodies with additional mitochondrial fluorescence. The higher resolution images of DHE (Fig. 5b) or Mitoethidium confirm this (Fig. 5c). It must be emphasized that the appearance of somatic and neuritic mitochondrial labeling in the presence of DHE does not indicate that the probe was oxidized within the matrix. As it is a membrane-permeant cation (Rottenberg 1984), a proportion of cytoplasmically generated ethidium may be accumulated by mitochondria, rather than binding to nuclear DNA.

Responsiveness to generated superoxide and cell permeant superoxide dismutase mimetics

Exogenous $O_2^{\cdot -}$ generated by xanthine/xanthine oxidase generates unphysiologically high concentrations of $O_2^{\cdot -}$ sufficient to produce a rapid increase in the oxidation of DHE (Fig. 6a), while with MitoSOX the increase in oxidation rate takes 20 min to become established (Fig. 6b), suggesting that there is limited accessibility of exogenous $O_2^{\cdot -}$ to the mitochondrial matrix. However, the cell-permeant superoxide dismutase mimetic Mn-TE-2-PyP is effective in competing for superoxide with both probes and reduces the basal levels of superoxide (Figs 6c and d).

Respiratory chain inhibitors and matrix superoxide levels

Rotenone and antimycin A increase superoxide levels in isolated mitochondria oxidizing Complex I substrates (St Pierre *et al.* 2002). Variable *in vitro* incubation conditions may account for the lack of consensus as to the effect of another Complex III inhibitor, myxothiazol (Raha *et al.* 2000; Starkov and Fiskum 2001). To validate the responsiveness of MitoSOX to endogenously generated matrix superoxide, CGNs were exposed to the inhibitors (Fig. 7). As the rate of increase in fluorescence is a linear function of the probe concentration in the medium (Fig. 4b), and thus its concentration in the matrix, it may be necessary to correct for changes in $\Delta\psi_m$ and $\Delta\psi_p$ that will affect the uptake of MitoSOX. In the case of the respiratory chain inhibitors, a partial depolarization of the mitochondria occurs as $\Delta\psi_m$ becomes supported by ATP synthase reversal (Nicholls 2006a). Previous studies with CGNs incubated under the same conditions reported a 26 mV drop in $\Delta\psi_m$ on addition of myxothiazol with no change in $\Delta\psi_p$(Nicholls 2006a). The present results (Fig. 7a) are consistent with this earlier determination: depolarizations varying from −17 mV (rote-

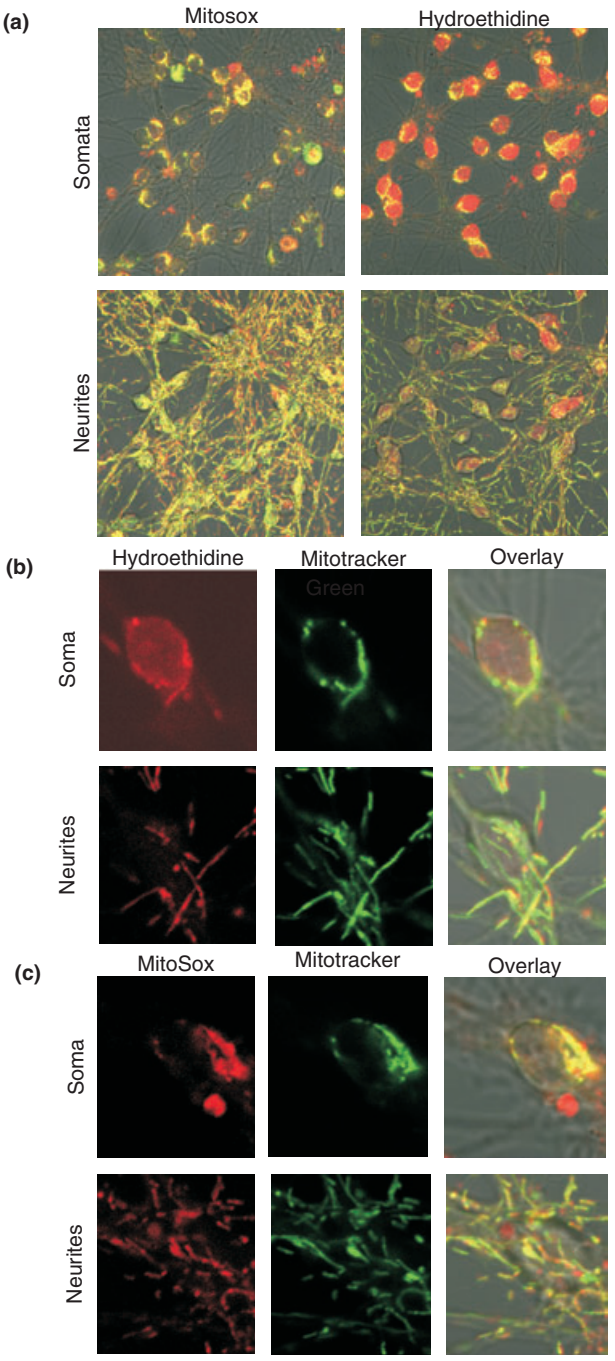

Fig. 5 Subcellular localization of the oxidation products of MitoSOX and DHE: cerebellar granule neurons were pre-incubated for 30 min with 100 nmol/L Mitotracker Green together with either 200 nmol/L MitoSOX or 200 nmol/L DHE. (a) wide-field image focusing on somata and neurites. Note the presence of Mitoethidium labeling in the nuclei of damaged cells. (b and c) high resolution images. Red, Mitoethidium or ethidium, green, Mitotracker.

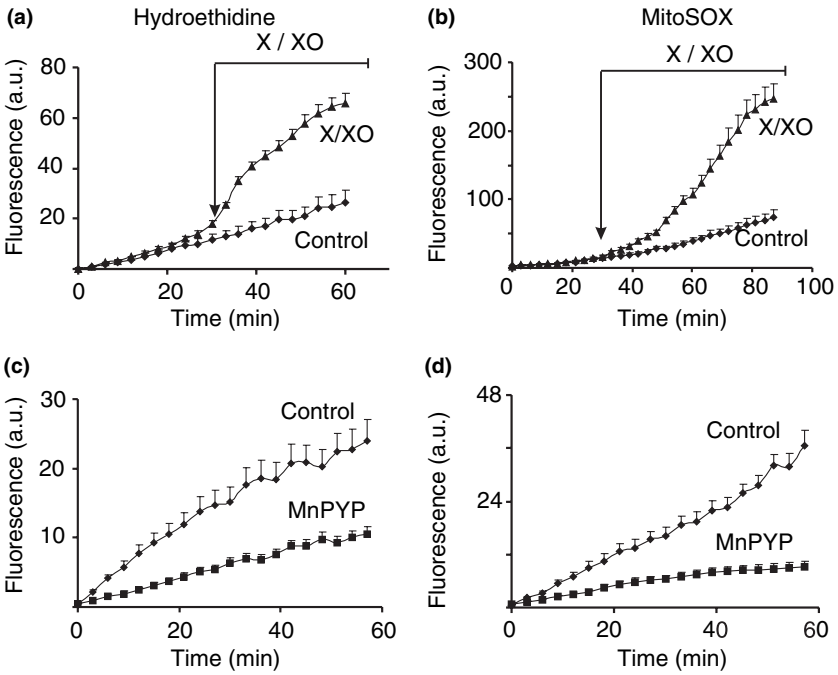

Fig. 6 Responsiveness of intracellular MitoSOX or DHE to extracellular generated superoxide and cell permeant superoxide dismutase mimetics: dihydroethidium (0.2 μmol/L) or MitoSOX (0.1 μmol/L) was added at $t = 0$. (a and b) xanthine (100 μmol/L) plus xanthine oxidase (14 mU/mL) were added at 30 min.Note the delayed increase in MitoSOX oxidation. (c and d) Mn-TE-PyP (50 μmol/L) was added at $t = 0$. Note the decrease in the rates of basal oxidation.

none) to −28 mV (myxothiazol) were determined. Fig. 7b reports the effects of the inhibitors on matrix superoxide in two ways. For each condition, ten cells were randomly selected. The rate of increase in Mitoethidium fluorescence was determined for each cell for the 30 min prior to addition of inhibitor and for a 30 min period starting 10 min after inhibitor addition, the delay allowing for any redistribution of MitoSOX. The mean ratio of the rates (after/before) is reported in Fig. 7b (solid bars). Because of the partial depolarization of the mitochondria the results in Fig. 7b have also been plotted after correcting for the estimated decrease in matrix MitoSOX concentration assuming that the concentration of the cationic MitoSOX parallels that of $TMRM^+$ as either membrane potential changes (open bars). The topology of $O_2^{\cdot -}$ release by Complex III is controversial but the present data supports observations that a significant proportion is released into the matrix (Brand 2005).

Proton conductance and matrix superoxide levels

The respirometer (Fig. 1) and $\Delta\psi_m$ traces (Fig. 2a) emphasize that it is important to distinguish between those low protonophore concentrations where some residual respiratory control is retained (i.e., 0–100 nmol/L in the present experiments) and concentrations that cannot be countered by an increase in respiration (250 nmol/L and above). As shown in Fig. 3c, the effect of the low concentrations is to increase respiration with only a very slight depression in $\Delta\psi_m$, whereas beyond the threshold for uncontrolled respiration $\Delta\psi_m$ drops rapidly as conductance cannot be compensated by any further increase in proton current. The rate of MitoSOX oxidation did not change significantly as FCCP increases within the respiratory control range (Fig. 8).

MitoSOX redistribution between matrix and cytoplasm

The large increase in Mitoethidium fluorescence following addition of 250 nmol/L FCCP (Fig. 8a) requires comment. In response to a large depolarization, sufficient MitoSOX would be predicted to redistribute from matrix to cytoplasm, allowing it to be oxidized by cytoplasmic O_2. The resulting Mitoethidium would be available to intercalate with nuclear DNA with further fluorescence enhancement. Fig. 9 shows that this redistribution can be seen with 250 nmol/L FCCP which causes a prolonged decay in $\Delta\psi_m$ (Fig. 2a and Nicholls 2006a). Thus MitoSOX is a valid monitor of matrix $O_2^{\cdot -}$ levels over a 30 mV range in $\Delta\psi_m$, after correction for its altered concentration in the matrix, but not for more extensive depolarizations where nuclear DNA becomes labeled. Redistribution to the nucleus was not seen with rotenone, antimycin a or myxothiazol (not shown) where $\Delta\psi_m$ stabilizes after decreasing by 17–28 mV (Fig. 7).

Proton conductance and cytoplasmic superoxide levels

Because DHE is uncharged it will not be selectively accumulated in the mitochondrial matrix. The dual localization of its oxidation product, ethidium, in the nucleus and mitochondria (Fig. 5) does not necessarily reflect the origin of its formation since a portion of the positively charged ethidium formed in the cytoplasm could be transported into the mitochondria rather than being bound by nuclear DNA. The rate of oxidation of DHE thus most likely represents cytoplasmic and inter-membrane superoxide lev-

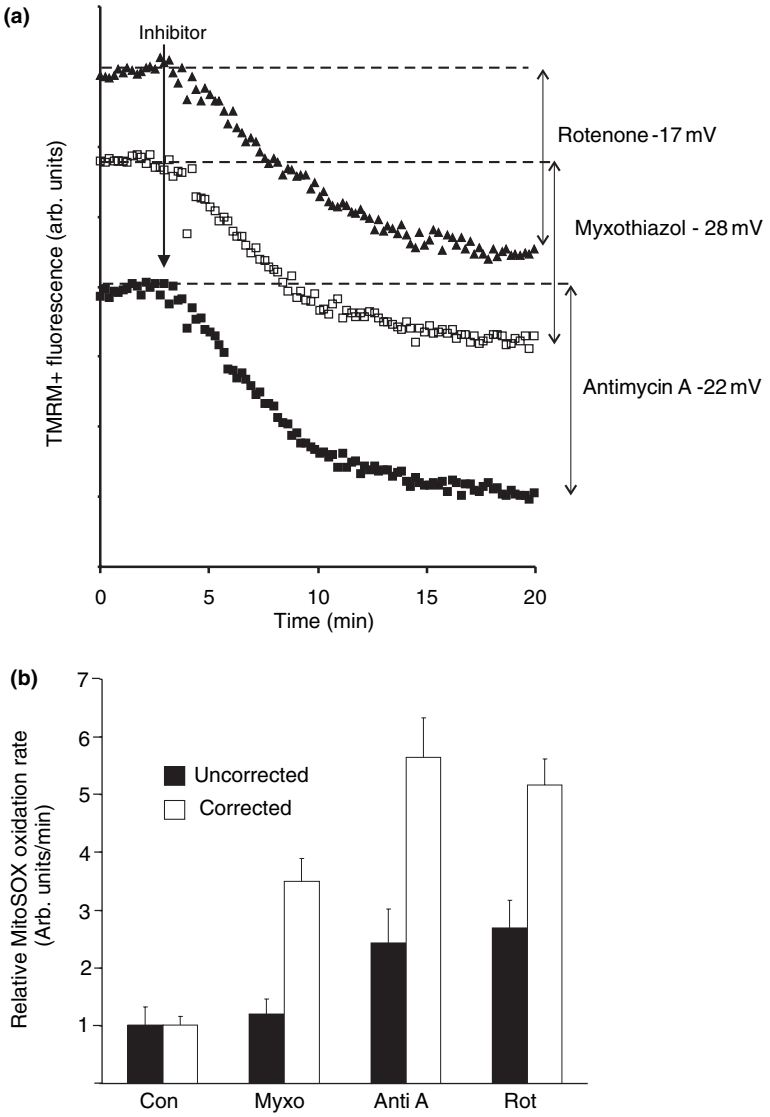

Fig. 7 Mitochondrial membrane potential changes and matrix superoxide on addition of respiratory chain inhibitors. (a) Cerebellar granule neurons were equilibrated with 5 nmol/L $TMRM^+$ (see Materials and methods). Where indicated 1 μmol/L rotenone, 1 μmol/L myxothiazol or 1 μmol/L antimycin A were added. Single cell fluorescence was monitored for a further 15 min. The decrease in $\Delta\psi_m$ was calculated using the program previously published (Nicholls 2006a). Traces are from a single representative cell body and the depolarizations are calculated from the mean of 10 somata. (b) A parallel experiment to the above was performed with cells pre-incubated for 30 min with 100 nmol/L MitoSOX prior to addition of the respiratory chain inhibitors. Histograms show relative matrix superoxide levels calculated from the slope of the fluorescence trace without (black bars) or with (white bars) correction for the decline in $\Delta\psi_m$.

els, perhaps generated by NADPH oxidase (Abramov *et al.* 2004). Over the range of FCCP concentrations that retain residual respiratory control the rate of DHE oxidation increases (Fig. 8b) in contrast to MitoSOX (Fig. 8a). When the respiratory control threshold is exceeded by 250 nmol/L FCCP, a further increase in superoxide is detected. Since the distribution of the uncharged DHE will be independent of $\Delta\psi_m$ no correction for changes in mitochondrial membrane potential are required.

Proton conductance and sensitivity to oxidative and excitotoxic stress

Although an increased mitochondrial proton conductance has been proposed to enhance neuroprotection by lowering levels of reactive oxygen species (Diano *et al.* 2003; Mattiasson *et al.* 2003; Andrews *et al.* 2005b; Conti *et al.* 2005), the results reported above suggest that the decrease in matrix superoxide levels in intact neurons is at best marginal. To test the consequences of mild uncoupling to counter oxidative stress, we employed two mitochondrially related oxidative stress paradigms: acute glutathione depletion (Fig. 10) which inhibits ATP export from the *in situ* mitochondria (Vesce *et al.* 2005) and mitochondrial-associated superoxide production by menadione redox cycling, Fig. 11. The low affinity fluo4FF only detects pathological increases in $[Ca^{2+}]_c$ following oxidative or excitotoxic DCD. To facilitate analysis regions of interest enclosing at least 100 cell bodies were analyzed. The increase in DCD, monitored by the Ca^{2+} indicated is mirrored by the decrease in $TMRM^+$ fluorescence reflecting a collapse in $\Delta\psi_m$ (Vesce *et al.* 2005). It is apparent that this concentration of FCCP, sufficient to utilize approximately 20% of the spare respiratory capacity of the neurons (Fig. 10) afforded no protection to the neurons. A similar experiment was performed in the presence of 10 μmol/L menadione to

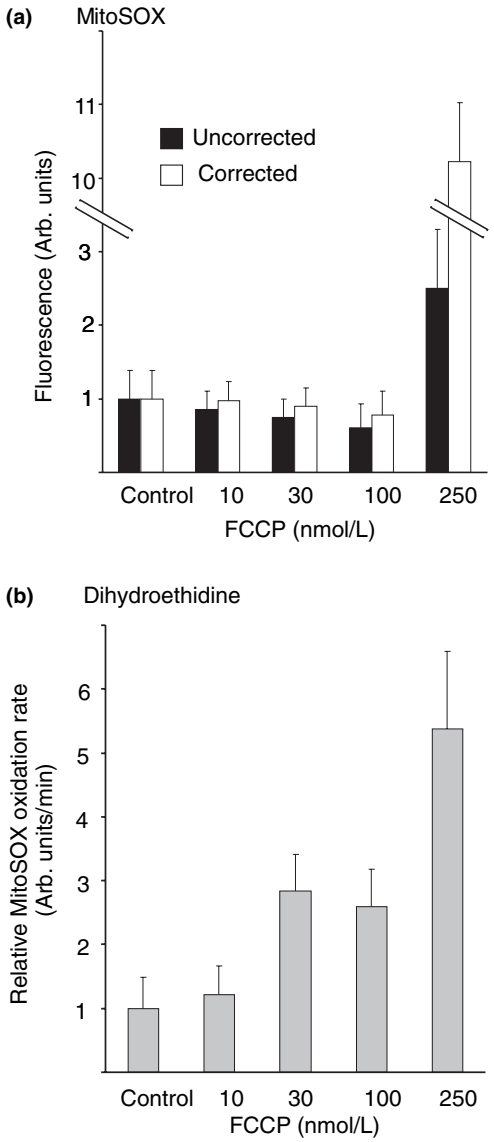

Fig. 8 Matrix and cytoplasmic superoxide levels as a function of protonophore concentration. (a) Cerebellar granule neurons (CGNs) equilibrated with 100 nmol/L MitoSOX were incubated with the indicated concentrations of FCCP. Superoxide levels detected by the rate of oxidation of MitoSOX are shown uncorrected for changes in $\Delta\psi_m$ (solid bars) or corrected for decreases in $\Delta\psi_m$ as determined in Fig. 3a. (b) CGNs were equilibrated with 100 nmol/L DHE and incubated in parallel.

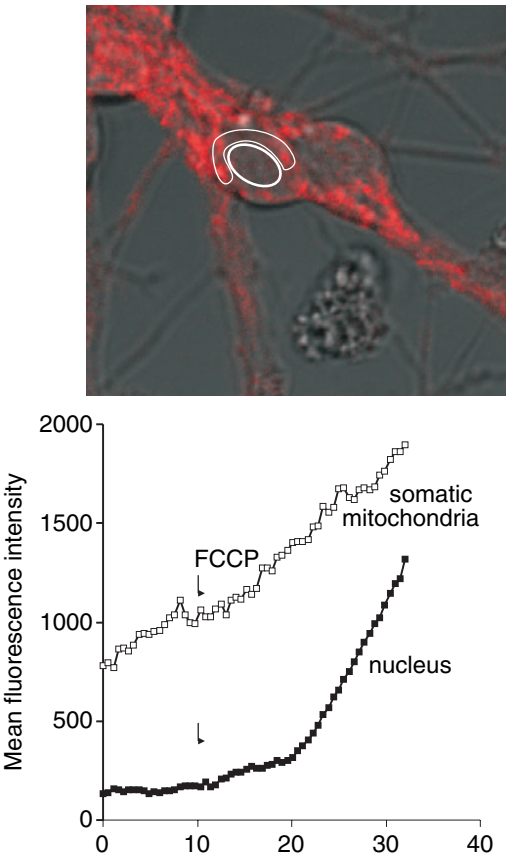

Fig. 9 Redistribution of MitoSOX in response to large mitochondrial depolarizations. Cerebellar granule neurons were equilibrated with 100 nmol/L MitoSox and mitochondria-rich and nuclear regions of a single neuron (outlined) were imaged. Where indicated 250 nmol/L carbonylcyanide-p-trifluoromethoxyphenyl hydrazone was added sufficient to induce a large mitochondrial depolarization (Fig. 2a). Note the delayed increase in nuclear fluorescence.

generate mitochondrially associated $O_2^{\cdot -}$ by redox cycling (Fig. 11). Here the presence of the protonophore significantly potentiated the toxic effect of the menadione.

Finally, the effect of low FCCP concentrations on the ability of CGNs to withstand prolonged NMDA receptor activation was determined (Fig. 12). As in the previous experiments an extended region of interest was used to quantify the fluo4FF fluorescence. The controlled increase in $[Ca^{2+}]_c$ induced by receptor activation prior to DCD is insufficient to produce a significant increase in fluorescence. No recovery of $[Ca^{2+}]_c$ in the deregulated cells was seen following addition of the NMDA receptor inhibitor MK-801 (not shown).

Discussion

The primary aim of this study was to test the hypothesis that subtle increases in inner mitochondrial membrane proton conductance, modeling the action of novel putative UCPs, could lower matrix superoxide levels and be neuroprotective in an *in vitro* model of glutamate excitotoxicity. While there is persuasive pathophysiological evidence that enhanced expression of UCP2 has a neuroprotective role (for review see Andrews *et al.* 2005a) much of the evidence for a protonophoric role of the protein in this context seems in conflict with established bioenergetic principles. The first problem is that an enhanced respiration diagnostic of an increased proton conductance is only reported in the presence of massive non-physiological concentrations of free fatty

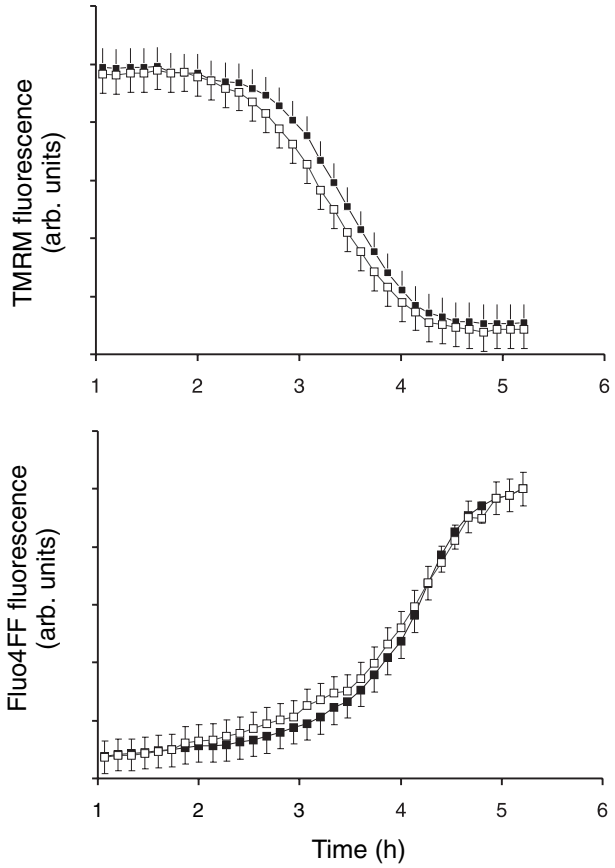

Fig. 10 Carbonylcyanide-p-trifluoromethoxyphenyl hydrazone (FCCP) (30 nmol/L) does not protect cerebellar granule neurons (CGNs) against delayed Ca^{2+} deregulation induced by glutathione depletion. CGNs were equilibrated with 5 nmol/L $TMRM^+$ and fluo4FF. At t = 0.100 μmol/L monochlorobimane was added to deplete glutathione (Vesce *et al.* 2005) in the presence (closed symbols) or absence (open symbols) of 30 nmol/L FCCP. From 1 h $TMRM^+$ and fluo4FF fluorescence was monitored from a region of interest comprising at least 100 neurons. The final time-points represented 100% deregulation. Results are the mean and SD of four experiments.

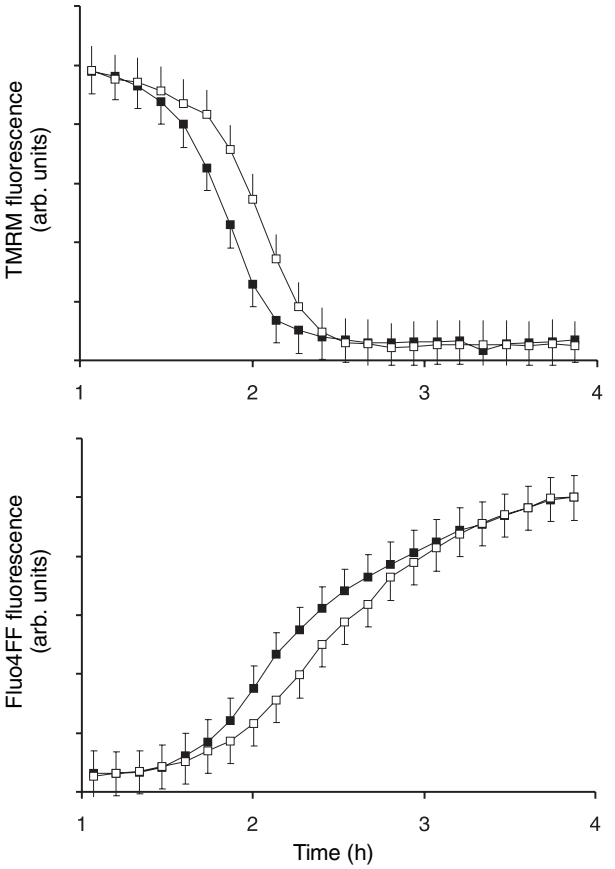

Fig. 11 Carbonylcyanide-p-trifluoromethoxyphenyl hydrazone (FCCP) (30 nmol/L) potentiates DCD in CGNs induced by menadione. CGNs were equilibrated with 5 nmol/L $TMRM^+$ and fluo4FF. At t = 0.10 μmol/L menadione was added in the presence (closed symbols) or absence (open symbols) of 30 nmol/L FCCP. From 1 h $TMRM^+$ and fluo4FF fluorescence was monitored from a region of interest comprising at least 100 neurons. The final time-points represented 100% deregulation. Results are the mean and SD of four experiments.

acid, i.e., 300 μmol/L palmitate in the presence of 16 μmol/L bovine serum albumin (Andrews *et al.* 2005b) or 30 μmol/L palmitate in the absence of albumin (Mattiasson *et al.* 2003). UCP2 over-expression is observed not to affect the basal state 4 respiration (and hence the proton leak) in the absence of palmitate (Mattiasson *et al.* 2003) and yet effects on ROS generation are reported in the absence of fatty acids (Mattiasson *et al.* 2003; Andrews *et al.* 2005b; Conti *et al.* 2005). The assumption in these studies is that, by extrapolation from observations with isolated mitochondria oxidizing succinate, low protonophoric activity will dramatically lower oxidative stress (Korshunov *et al.* 1997; Votyakova and Reynolds 2001; Lambert and Brand 2004). However, mitochondria within intact cells are never in the position of purely oxidizing substrates that feed directly into the UQ pool. Thus succinate is generated (and fumarate removed) by NADH-linked dehydrogenases feeding into Complex I. It follows that the supra maximal Δp seen with isolated mitochondria with UQ-linked substrates (Nicholls 1977) does not normally occur in real cells. Importantly, the rate of superoxide generation by isolated mitochondria with NADH-linked substrates is far lower (Brand *et al.* 2004; Tretter and Adam-Vizi 2007). In intact isolated nerve terminals (synaptosomes) superoxide levels are low and insensitive to additions of uncouplers (Sipos *et al.* 2003). The present results are consistent with this study, and illustrate clearly the pitfalls in directly extrapolating from isolated mitochondrial studies that do not mimic the *in situ* physiology.

Oxidative stress and glutamate excitotoxicity

There is a clear association between oxidative stress and the susceptibility of cultured neurons to glutamate excitotoxicity

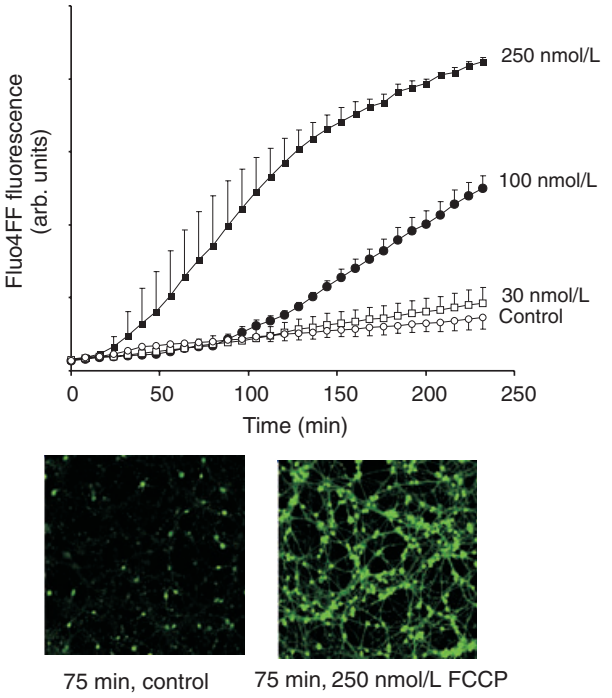

Fig. 12 Carbonylcyanide-p-trifluoromethoxyphenyl hydrazone (FCCP) enhances DCD induced by chronic NMDA receptor activation. Cerebellar granule neurons were pre-incubated for 1 h with 0.5 μmol/L fluo4FF. At $t = 0.200$ μmol/L glutamate plus 20 μmol/L glycine were added in the presence of varying FCCP concentrations. Fluo4FF fluorescence was monitored from regions of interest comprising at least 100 neurons. The final time-points with 250 nmol/L FCCP represented 100% deregulation. Results are the mean and SD of four experiments. Representative fields are shown 75 min after glutamate addition in the absence and presence of 250 nmol/L FCCP.

[reviewed in Nicholls (2004)]. The standard hypothesis has been that calcium loaded mitochondria resulting from pathological NMDA receptor activation generate excess reactive oxygen species that damage the mitochondria and lead to cell death. While this hypothesis is supported by results showing an increase in reactive oxygen species following NMDA receptor activation, single cell analysis shows that this occurs only once the cell has initiated DCD (Vesce *et al.* 2004). However, it is also apparent that oxidative damage to the *in situ* mitochondria sufficient to restrict their capacity to export ATP greatly potentiates the susceptibility of the cells to DCD (Vesce *et al.* 2005). A similar relationship is apparent in the present context of controlled uncoupling. NMDA receptor activation substantially increases the ATP demand of the mitochondria, primarily because of the activation of the Na^+/K^+-ATPase by Na^+ entering through the receptor (Jekabsons and Nicholls 2004). Any increase in proton conductance proportionately decreases the maximal ATP generating capacity of the mitochondria by syphoning off part of the proton current through the leak instead of the ATP synthase (Fig. 1), and stochastic cell death seems to result whenever a cell's ATP demand cannot be met by the mitochondria and glycolysis. The failure of cell permeant antioxidants to protect against DCD (Vesce *et al.* 2004) also supports the hypothesis that insufficient ATP generating capacity rather than oxidative stress is a more direct cause of DCD.

The exact event precipitating DCD is still debated. Mitochondrial Ca^{2+} overload is clearly implicated (White and Reynolds 1995; Ward *et al.* 2000) although CGNs undergo glutamate-mediated DCD in media where Sr^{2+} is substituted for Ca^{2+} (Wabnitz *et al.* 2006). However, Sr^{2+} does not induce a permeability transition in isolated mitochondria (Bernardi *et al.* 1992). Additionally, there is controversy as to whether the mitochondrial permeability pore inhibitor cyclosporin A does (Nieminen *et al.* 1996; Schinder *et al.* 1996; White and Reynolds 1996; Vergun *et al.* 1999) or does not (Castilho *et al.* 1998; Isaev *et al.* 1998; Chinopoulos *et al.* 2004) confer significant protection in this model. Paradoxically, in neuronal preparations possessing high glycolytic capacity, extensive mitochondrial depolarization by the combination of rotenone plus oligomycin (Budd and Nicholls 1996; Castilho *et al.* 1998) or brief exposure to high protonophore concentrations (Stout *et al.* 1998; Mattiasson *et al.* 2003; Pivovarova *et al.* 2004; Korde *et al.* 2005) during glutamate exposure can protect the cells against DCD. Under these conditions the mitochondria do not accumulate Ca^{2+} (Budd and Nicholls 1996) and glycolysis in these preparations is sufficiently active to maintain ATP levels in the absence of oxidative phosphorylation (Budd and Nicholls 1996).

Matrix superoxide levels

As DHE is uncharged, it should be present at roughly equal concentrations in the cytoplasm and the mitochondrial matrix and therefore detect superoxide in both compartments. The availability of MitoSOX, a derivative of DHE conjugated to triphenylphosphonium, opens the possibility for the direct monitoring of superoxide levels inside the mitochondrial matrix in intact cultured neurons. This study indicates that the probe is a valid monitor of matrix superoxide levels as long as its concentration within the matrix is controlled for changes in plasma or mitochondrial membrane potentials, and as long as the concentration of the oxidized Mitoethidium is sufficiently low to allow its intercalation into mitochondrial DNA. The present studies indicate that when respiratory chain inhibitors are added, and when low concentrations of FCCP induce subtle changes in mitochondrial membrane potential, it may be important to correct for the altered concentration of MitoSox within the mitochondrial matrix. The assumption is made that the distribution of MitoSox across both the plasma and mitochondrial membranes is proportional to that of the cationic $TMRM^+$. Failure to make such a correction could lead to an underestimation of superoxide levels under conditions where there is a partial depolarization of either membrane.

The relation between proton conductance and mitochondrial membrane potential

The rate of electron flow through the proton pumping complexes is a function of the thermodynamic disequilibrium between the redox span and the protonmotive force. As the effective proton conductance of the membrane increases, e.g., following FCCP addition, Δp falls and electron transport accelerates. Previous studies with isolated mitochondria showed that Δp decreased by only about 10% between state 4 (zero ATP turnover) and state 3 (maximal ATP turnover) (Nicholls and Bernson 1977). Present results for *in situ* mitochondria (Fig. 2) shows that $\Delta\psi_m$ changes by less than 2% as FCCP is titrated in until respiratory capacity is reached. It is apparent that a critical threshold exists for protonophore addition, beyond which increased respiratory activity is unable to compensate for the increased C_mH^+. As a result $\Delta\psi_m$ falls precipitately . In the present design this occurs between 100 nmol/L and 250 nmol/L FCCP (see Figs 1, 2, 8 and 9).

In low potassium medium the basal respiration of the CGN's accounts for about 30% of the mitochondrial respiratory capacity (Jekabsons and Nicholls 2006), thus the mitochondria are closer to state 4 than state 3. The very slight change in membrane potential as FCCP is titrated in may underestimate the change in total protonmotive force since the pH gradient is not determined, and the matrix will be progressively acidified by the addition of the protonophore. In the basal state addition of the K^+/H^+ antiport ionophore nigericin hyperpolarizes the membrane potential by about 30 mV, consistent with the dissipation of the pH gradient of about −0.5 units (Nicholls 2006a). Nevertheless, the present results indicate that the *in situ* mitochondria possess homeostatic mechanisms that minimize the energy dependent drop in membrane potential. This clearly does not favor a mechanism in which an increased proton conductance is utilized to decrease membrane potential and restrict the generation of reactive oxygen species.

All mitochondria possess an endogenous proton leak that is regulated by Δp [reviewed in Brand (2005)]. The leak is particularly apparent with 'hyper-polarizing' substrates that feed electrons directly into the UQ pool. With isolated mitochondria the leak is greatly reduced in state 3, and may therefore act to limit the supra-maximal Δp that may be achieved by such substrates. It is significant that the Δp at which the endogenous proton leak becomes activated is close to that reported for the activation of superoxide generation during succinate oxidation by isolated mitochondria. As all mitochondria possess this voltage gated proton leak, it is not immediately apparent why an additional, UCP-mediated, mechanism would be required to limit $\Delta\psi_m$ and superoxide generation.

Conclusion

In the present model of glutamate excitotoxicity the classic 'uncoupling' effects of low protonophore concentrations, namely an increase in proton conductance and respiration and a proportionate decrease in the spare respiratory capacity available for peak demands for ATP synthesis, for example to extrude the Na^+ entering via a pathologically activated NMDA receptor, greatly outweigh any marginal decrease in matrix superoxide levels. This study indicates that aspects of the 'mild uncoupling' hypothesis, whereby novel UCPs are proposed to be neuroprotective, may need to be re-examined in view of the fact that the dominant effect of uncouplers is to uncouple ATP synthesis from electron transport.

References

Abramov A. Y., Canevari L. and Duchen M. R. (2004) β-amyloid peptides induce mitochondrial dysfunction and oxidative stress in astrocytes and death of neurons through activation of NADPH oxidase. *J. Neurosci.* **24**, 565–575.

Andrews Z. B., Diano S. and Horvath T. L. (2005a) Mitochondrial uncoupling proteins in the CNS: in support of function and survival. *Nat. Rev. Neurosci.* **6**, 829–840.

Andrews Z. B., Horvath B., Barnstable C. J., Elseworth J., Yang L. C., Beal M. F., Roth R. H., Matthews R. T. and Horvath T. L. (2005b) Uncoupling protein-2 is critical for nigral dopamine cell survival in a mouse model of Parkinson's disease. *J. Neurosci.* **25**, 184–191.

Beal M. F. (1995) Aging, energy, and oxidative stress in neurodegenerative diseases. *Ann. Neurol.* **38**, 357–366.

Beal M. F. (1996) Mitochondria, free radicals, and neurodegeneration. *Curr. Opin. Neurobiol.* **6**, 661–666.

Bernardi P., Vassanelli S., Veronese P., Colonna R., Szabo I. and Zoratti M. (1992) Modulation of the mitochondrial permeability transition pore. Effect of protons and divalent cations. *J Biol Chem.* **267**, 2934–2939.

Brand M. D. (2005) The efficiency and plasticity of mitochondrial energy transduction. *Biochem. Soc. Trans.* **33**, 897–904.

Brand M. D., Affourtit C., Esteves T. C., Green K., Lambert A. J., Miwa S., Pakay J. L. and Parker N. (2004) Mitochondrial superoxide: production, biological effects, and activation of uncoupling proteins. *Free Radic. Biol. Med.* **37**, 755–767.

Budd S. L. and Nicholls D. G. (1996) Mitochondrial calcium regulation and acute glutamate excitotoxicity in cultured cerebellar granule cells. *J. Neurochem.* **67**, 2282–2291.

Castilho R. F., Hansson O., Ward M. W., Budd S. L. and Nicholls D. G. (1998) Mitochondrial control of acute glutamate excitotoxicity in cultured cerebellar granule cells. *J. Neurosci.* **18**, 10 277–10 286.

Chinopoulos C., Gerencser A. A., Doczi J., Fiskum G. and dam-Vizi V. (2004) Inhibition of glutamate-induced delayed calcium deregulation by 2-APB and La^{3+} in cultured cortical neurones. *J Neurochem.* **91**, 471–483.

Conti B., Sugama S., Lucero J. *et al.* (2005) Uncoupling protein 2 protects dopaminergic neurons from acute 1,2,3,6-methyl-phenyltetrahydropyridine toxicity. *J. Neurochem.* **93**, 493–501.

Courtney M. J., Lambert J. J. and Nicholls D. G. (1990) The interactions between plasma membrane depolarization and glutamate receptor activation in the regulation of cytoplasmic free calcium in cultured cerebellar granule cells. *J. Neurosci.* **10**, 3873–3879.

Coyle J. T. and Puttfarcken P. S. (1993) Oxidative stress, glutamate and neurodegenerative disorders. *Science* **262**, 689–695.

Diano S., Matthews R. T., Patrylo P., Yang L., Beal M. F., Barnstable C. J. and Horvath T. L. (2003) Uncoupling protein 2 prevents neuronal death including that occurring during seizures: a mechanism for preconditioning. *Endocrinology* **144**, 5014–5021.

Dugan L. L., Sensi S. L., Canzoniero L. M. T., Handran S. D., Rothman S. M., Lin T. S., Goldberg M. P. and Choi D. W. (1995) Mito-

chondrial production of reactive oxygen species in cortical neurons following exposure to NMDA. *J. Neurosci.* **15**, 6377–6388.

Horvath T. L., Diano S. and Barnstable C. (2003) Mitochondrial uncoupling protein 2 in the central nervous system: neuromodulator and neuroprotector. *Biochem. Pharmacol.* **65**, 1917–1921.

Isaev N. K., Stelmashook E. V., Alexandrova O. P., Andreeva N. A., Polyakova I. A., Victorov I. V. and Zorov D. B. (1998) The lack of extracellular Na^+ exacerbates Ca^{2+}-dependent damage of cultured cerebellar granule cells. *FEBS Lett.* **434**, 188–192.

Jekabsons M. B. and Nicholls D. G. (2004) *In situ* respiration and bioenergetic status of mitochondria in primary cerebellar granule neuronal cultures exposed continuously to glutamate. *J. Biol. Chem.* **279**, 32 989–33 000.

Jekabsons M. B. and Nicholls D. G. (2006) Bioenergetic analysis of cerebellar granule neurons undergoing apoptosis by potassium/serum deprivation. *Cell Death Differ.* **13**, 1595–1610.

Korde A. S., Pettigrew L. C., Craddock S. D. and Maragos W. F. (2005) The mitochondrial uncoupler 2,4-dinitrophenol attenuates tissue damage and improves mitochondrial homeostasis following transient focal cerebral ischemia. *J. Neurochem.* **91**, 257–262.

Korshunov S. S., Skulachev V. P. and Starkov A. A. (1997) High protonic potential actuates a mechanism of production of reactive oxygen species in mitochondria. *FEBS Lett.* **416**, 15–18.

Lambert A. J. and Brand M. D. (2004) Superoxide production by NADH: ubiquinone oxidoreductase (complex I) depends on the pH gradient across the mitochondrial inner membrane. *Biochem. J.* **382**, 511–517.

Mattiasson G., Shamloo M., Gido G. *et al.* (2003) Uncoupling protein-2 prevents neuronal death and diminishes brain dysfunction after stroke and brain trauma. *Nature Med.* **9**, 1062–1068.

Nedergaard J. and Cannon B. (2003) The 'novel' 'uncoupling' proteins UCP2 and UCP3: what do they really do? Pros and cons for suggested functions *Exp. Physiol* **88**, 65–84.

Nicholls D. G. (1977) The effective proton conductances of the inner membrane of mitochondria from brown adipose tissue: dependency on proton electrochemical gradient. *Eur. J. Biochem.* **77**, 349–356.

Nicholls D. G. (2004) Mitochondrial dysfunction and glutamate excitotoxicity studied in primary neuronal cultures. *Curr. Mol. Med.* **4**, 149–177.

Nicholls D. G. (2006a) Simultaneous monitoring of ionophore- and inhibitor-mediated plasma and mitochondrial membrane potential changes in cultured neurons. *J. Biol. Chem.* **281**, 14 864–14 874.

Nicholls D. G. (2006b) The physiological regulation of uncoupling proteins. *Biochim. Biophys. Acta Bio-Energetics* **1757**, 459–466.

Nicholls D. G. and Bernson V. S. M. (1977) Inter-relationships between proton electrochemical gradient, adenine nucleotide phosphorylation potential and respiration during substrate-level and oxidative phosphorylation by mitochondria from brown adipose tissue of cold-adapted guinea-pigs. *Eur. J. Biochem.* **75**, 601–612.

Nicholls D. G., McLaughlin M. and Budd D. C. (1998) Metabotropic glutamate receptors, protein kinase C and the control of glutamate exocytosis, in *Metabotropic Glutamate Receptors and Brain Function* (Moroni F., Nicoletti F. and Pellegrini D., eds), pp. 179–190. Portland Press, London.

Nieminen A. L., Petrie T. G., Lemasters J. J. and Selman W. R. (1996) Cyclosporin a delays mitochondrial depolarization induced by *N*-methyl-D-aspaparte in cortical neurons: evidence of the mitochondrial permeability transition. *Neurosci.* **75**, 993–997.

Pivovarova N. B., Nguyen H. V., Winters C. A., Brantner C. A., Smith C. L. and Andrews S. B. (2004) Excitotoxic calcium overload in a subpopulation of mitochondria triggers delayed death in hippocampal neurons. *J. Neurosci.* **24**, 5611–5622.

Raha S., McEachern G. E., Myint A. T. and Robinson B. H. (2000) Superoxides from mitochondrial complex III: the role of manganese superoxide dismutase. *Free Radic. Biol. Med.* **29**, 170–180.

Rego A. C. and Oliveira C. R. (2003) Mitochondrial dysfunction and reactive oxygen species in excitotoxicity and apoptosis: Implications for the pathogenesis of neurodegenerative diseases. *Neurochem. Res.* **28**, 1563–1574.

Reynolds I. J. and Hastings T. G. (1995) Glutamate induces the production of reactive oxygen species in cultured forebrain neurons following NMDA receptor activation. *J. Neurosci.* **15**, 3318–3327.

Rottenberg H. (1984) Membrane potential and surface potential in mitochondria: uptake and binding of lipophilic cations. *J. Membr. Biol.* **81**, 127–138.

Rousset S., Alves-Guerra M. C., Mozo J., Miroux B., Cassard-Doulcier A. M., Bouillaud F. and Ricquier D. (2004) The biology of mitochondrial uncoupling proteins. *Diabetes* **53**, S130–S135.

Schinder A. F., Olson E. C., Spitzer N. C. and Montal M. (1996) Mitochondrial dysfunction is a primary event in glutamate excitotoxicity. *J. Neurosci.* **16**, 6125–6133.

Sengpiel B., Preis E., Krieglstein J. and Prehn J. H. M. (1998) NMDA-induced superoxide production and neurotoxicity in cultured rat hippocampal neurons: role of mitochondria. *Eur. J. Neurosci.* **10**, 1903–1910.

Sipos I., Tretter L. and Adam-Vizi V. (2003) The production of reactive oxygen species in intact isolated nerve terminals is independent of the mitochondrial membrane potential. *Neurochem. Res.* **28**, 1575–1581.

St Pierre J., Buckingham J. A., Roebuck S. J. and Brand M. D. (2002) Topology of superoxide production from different sites in the mitochondrial electron transport chain. *J. Biol. Chem.* **277**, 44 784–44 790.

Starkov A. A. and Fiskum G. (2001) Myxothiazol induces H_2O_2 production from mitochondrial respiratory chain. *Biochem. Biophys. Res. Commun.* **281**, 645–650.

Stout A. K., Raphael H. M., Kanterewicz B. I., Klann E. and Reynolds I. J. (1998) Glutamate-induced neuron death requires mitochondrial calcium uptake. *Nature Neurosci.* **1**, 366–373.

Tretter L. and Adam-Vizi V. (2007) Moderate dependence of ROS formation on DeltaPsim in isolated brain mitochondria supported by NADH-linked substrates. *Neurochem. Res.* (in press).

Vergun O., Keelan J., Khodorov B. I. and Duchen M. R. (1999) Glutamate-induced mitochondrial depolarization and perturbation of calcium homeostasis in cultured rat hippocampal neurones. *J. Physiol. (Lond.)* **519**, 451–466.

Vesce S., Kirk L. and Nicholls D. G. (2004) Relationships between superoxide levels and delayed calcium deregulation in cultured cerebellar granule cells exposed continuously to glutamate. *J. Neurochem.* **90**, 683–693.

Vesce S., Jekabsons M. B., Johnson-Cadwell L. I. and Nicholls D. G. (2005) Acute glutathione depletion restricts mitochondrial ATP export in cerebellar granule neurons. *J. Biol. Chem.* **280**, 38 720–38 728.

Votyakova T. V. and Reynolds I. J. (2001) $Deltapsi_m$-dependent and -independent production of reactive oxygen species by rat brain mitochondria. *J. Neurochem.* **79**, 266–277.

Wabnitz A. V., Storozhevykh T. P., Senilova Y. E., Pinelis V. G. and Khodorov B. I. (2006) The permeability transition pore is not a prerequisite for glutamate-induced calcium deregulation and mitochondrial depolarization in brain neurons. *Biol. Membranes* **22**, 346–350.

Ward M. W., Rego A. C., Frenguelli B. G. and Nicholls D. G. (2000) Mitochondrial membrane potential and glutamate excitotoxicity in cultured cerebellar granule cells. *J. Neurosci.* **20**, 7208–7219.

White R. J. and Reynolds I. J. (1995) Mitochondria and Na^+/Ca^{2+} exchange buffer glutamate- induced calcium loads in cultured cortical neurons. *J. Neurosci.* **15**, 1318–1328.

White R. J. and Reynolds I. J. (1996) Mitochondrial depolarization in glutamate-stimulated neurons: An early signal specific to excitotoxin exposure. *J. Neurosci.* **16**, 5688–5697.

